SCIENTIFIC BULLETIN OF THE LODZ UNIVERSITY OF TECHNOLOGY
No. 1210 Physics, Vol. 37 2016

SYLWESTER KANIA[1,2], BARBARA KOŚCIELNIAK-MUCHA[2] JANUSZ KULIŃSKI[2,3], PIOTR SŁOMA[2], KRZYSZTOF WOJCIECHOWSKI[2]

[1] Institute of Physics, Lodz University of Technology, ul. Wólczańska 219 90-924, Łódź, Poland
[2] Centre of Mathematics and Physics, Lodz University of Technology Al. Politechniki 11, 90-924 Łódź, Poland
[3] The Faculty of Mathematics and Natural Sciences, Jan Długosz University in Częstochowa, Al. Armii Krajowej 13/15, 42-218 Częstochowa, Poland

THE EFFECT OF SYMMETRY OF A MOLECULE ELECTRONIC DENSITY ON THE DIPOLE MOMENT OF UNIT CELL AND HOLE CONDUCTIVITY OF THIN POLYCRYSTALLINE FILMS OF ANTHRONE AND ANTHRAQUINONE

The electronic structure of anthrone and anthraquinone molecules in the gas state and in the simulated crystal unit cell were calculated with time dependent-density functional theory (TD-DFT) method. The values of dipole moment of single molecule and of single crystal unit cell were also determined with TD-DFT method. The results of TD-DFT were compared with known crystal structures of both compounds [1,2]. For both molecules it was observed improvement of matching the length of corresponding bonds when calculated for the unit cell. Unexpectedly high value of dipole moment was calculated for the single unit cell of anthrone. This fact can be responsible for the nano-dimension properties of anthrone as the carriers mobility or high boiling point.

Keywords: anthrone, anthraquinone, TD-DFT, hole drift mobility, carrier transport, dipole moment, polycrystalline films.

1. INTRODUCTION

The range of possible applications of organic semiconducting materials is wide. One can mention electronic switches, batteries, light emitting diodes and Schottky diodes, field effect transistors, solar cells as the most important applications [3,4,5]. Such wide application of these materials is associated with the continuous investigations of their properties.

The characteristic feature of organic molecules is flexibility of designing molecular material optimally adapted to desired characteristic of their properties. The adequate arrangement of the condensed rings and substituents is possible due to the prior analysis based on a knowledge of the desirable electrical and mechanical properties of the material. Investigations of the crystalline structure and theoretical predictions with use of molecular structure calculations are very helpful. However, the variety of phenomena that affect the conduction imply that the results of theoretical calculations must always be tested experimentally. The well-known theories can only partly explain the experimental results.

The efficiency of charge transport through the film is largely influenced by the degree of molecular organization. The most common intermolecular interactions that contribute to molecular packing are the π-π and C-H-π interactions, commonly found in acenes and tiophenes derivatives [6].

When neutral organic molecule is charged during hole type transport, it forms cationic open - shell electronic configuration [7] corresponding to:

$$M \rightarrow M^{+} + e^{-}. \tag{1}$$

The energy change connected with this charge transfer is called the internal reorganization energy (λ^{int}). Electronic polarization of surrounding molecules is connected with external reorganization energy (λ^{ext}).

The energy of the reorganization is closely related to the transport of charge carriers. The source of the creation of this energy is a geometric relaxation of the distribution of electron density in the volume of material associated with the charge transfer and described by an effective electronic coupling matrix element (J_{ij}) between neighbouring molecules, dictated largely by orbital overlap. Fig. 1 illustrates the meaning of the reorganization energy considered in connection with the elementary hopping step.

The total reorganization energy between *i* and *j* molecule may be described as a sum of internal and external terms [8] characterized by four energies [9]: *E* (neutral molecule in neutral molecule geometry), *E** (neutral molecule in ion geometry), E^{*}_{+} (ion in ion geometry), and E_{+} (ion in neutral geometry).

$$\lambda_{ij} = \lambda_{ij}^{\text{int}} + \lambda_{ij}^{ext} = \left(E^{*}_{+} - E_{+}\right) + \left(E^{*} - E\right) \tag{2}$$

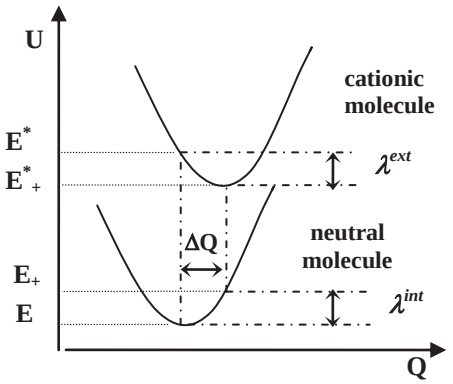

Fig. 1. Schematic representation of the potential energy surfaces of the neutral and cationic molecules (Q – reaction coordinate, U – potential energy)

The susceptibility in respect to the intramolecular structure of the molecules and the structure in their co-ordination sphere on the deformations is caused by moving the charge carriers. More detailed studies [10,11] reveal a strong correlation between the localization of the charge carriers and their reorganization energy in organic molecular crystals. Small reorganization energies are usually associated with a strong delocalization of charge carriers. Delocalization of charge carriers enables to obtain larger mobilities due to reduced dependence of the conductivity on thermal fluctuations of the geometry of the entire system.

It leads to the problem of relationship between the symmetry of electron density of the molecule and transport properties of thin layer built of these molecules [6,7,8,12].

In the high temperature limit, the transfer rate for a charge to hop from a site *i* to a final site *j* for aromatic compounds is [8,13]:

$$k_{ij} = \frac{2\pi}{\hbar} \frac{J_{ij}^2}{\sqrt{4\pi\lambda_{ij} k_B T}} \exp\left[-\frac{\left(\Delta E_{ij} - \lambda_{ij}\right)^2}{4\lambda_{i\alpha} k_B T} \right], \tag{3}$$

where T is temperature, k_B is the Boltzmann constant, ΔE_{ij} – is difference of electron energy between the initial and final molecular sites, $\hbar$ -is the reduced Planck constant, J_{ij} – is a transfer integral describing electron transfer from molecule *i* to molecule *j*.

The theoretical description of the conductivity of the molecular systems needs the understanding of the fact that nuclear dynamics is much slower than the dynamics of charge carriers and that the electronic coupling is weak. This

situation enables to divide the whole system to the subsystems, and to present the Hamiltonian operator describing the whole system as a sum of terms.

For molecular systems coupling calculations are commonly made using density functional theory (DFT). Applying the self-consistent formalism to construct the Kohn-Sham-Fock operator for dimer interactions with assumption that HOMO (high occupied orbital) and HOMO-1 of the dimer results only from the interaction of the monomers HOMO. The secular equation for dimer molecular orbitals and the corresponding dimer orbital energies can be described in the form:

$$\boldsymbol{HC} - E\boldsymbol{SC} = 0, \tag{4}$$

where $\boldsymbol{H}$ and $\boldsymbol{S}$ are the Hamiltonian and overlapping matrices of the system, and C and E are the Kohn-Sham molecular orbital coefficients and eigenstates of the non-interacting dimer, respectively.

Dipole-dipole interactions energy between the dipole $\vec{s}_1$ placed in the centre of the coordinate system having direction s_1 in the field originated from the network of point dipoles with manifold of directions s_n can be described in the form of the sum of interactions with all other dipoles [18]:

$$\delta J_{1\alpha} = \frac{d^2}{2} \sum_{n=2}^{\infty} \left[\frac{\vec{s}_1 \vec{s}_n}{\left|\vec{r}_{1n}\right|^3} - \frac{3(\vec{s}_1 \vec{r}_{1n})(\vec{s}_n \vec{r}_{1n})}{\left|\vec{r}_{1n}\right|^5} \right], \tag{5}$$

where: r_{1n} is a position of n-th dipole, α-sign a manifold of the network of point dipoles. This energy for solid anthraquinone, with the molecules without significant natural dipole moment is of the order of 10^{-5}-10^{-6} eV, that is much less than the van der Waals potential energy (estimated for this material in the range of 10^{-3}-$7 \cdot 10^{-2}$ eV). For anthrone molecules with a significant natural dipole moment of 3,5 D ($1{,}19 \cdot 10^{-29}$ Cm) (in benzene) [14] the energy of dipole-dipole interaction can be as much as 10^{-3}-10^{-2} eV, that is the value comparable to the van der Waals potential. These additional dipole-dipole energies present for anthrone structures can lead to increase of the interactions between anthrone molecules in the condensed state (in comparison to the anthraquinone molecules) and to the enlarging overlapping of the wave functions what is favourable to enhance conduction of the charge carriers via localized states.

Our research is related to thin films of two compounds, i.e. anthrone and anthraquinone built on the basis of anthracene skeleton, with the molecular weight for anthrone MW = 194,228 g/mol and for anthraquinone MW = 208,212 g/mol. In Table 1, density, molecular weight, melting point and boiling point of these materials are presented in relation to the same properties of anthracene, i.e. the compound of which these materials are derivatives.

Both mentioned above compounds crystallize in the nearly identical crystal lattices [16], monoclinic system with point group C_{2h}^5 and space group ($P2_1/a$) with bimolecular unit of the dimensions (at 20°C): a_0 = (15,83±0.04) Å, b_0 = (3,97±0.01) Å, c_0 = (7,89±0.01)Å, β =102,5° for anthraquinone [2], and a_0 = (15.80±0.03) Å, b_0 = (3.998±0.005) Å, c_0 = (7.860±0.016) Å, β = 101° 40'±10', Z = 2 for anthrone [1]. The main difference, essential for our studies, is the fact that the anthraquinone molecules being centrosymmetric possess small dipole moment in solution, near zero [14], opposite to the non-centrosymmetric anthrone molecules which are characterised by large dipole moment of 3,5 D [14].

Table1

Basic properties of anthrone and anthraquinone in comparison to anthracene [15,16] (MW-molecular weight, Mp-melting point, Bp-boiling point, d-density)

	anthrone ($C_{14}H_{10}O$)	anthraquinone ($C_{14}H_8O_2$)	anthracene ($C_{14}H_{10}$)
CAS number	90-44-8	84-65-1	120-12-7
MW. [g/mol]	194.228	208.212	178.229
Mp [K]	428	559	483
Bp [K]	994	653	613
d [g/cm^3]	1,33	1,44	1,28

The X-ray analysis of the structure of solid anthrone demonstrates appearance of the diffuse layers for the planes (100) and (001) [17], what results in appearance of the symmetry of the unit cell identical to the anthraquinone unit cell. It is surprising because the molecules of anthrone have a lower symmetry. This property may be attributed to the statistical disorder for the direction and sense of dipole moment vector which are strictly correlated with the position of the oxygen atom in the neighbouring molecules. In the row of molecules parallel to [010] direction, the molecules regularly change their direction and sense of dipole moment. Calculation of the dipole interaction in the crystalline anthrone made for the pair of molecules inverted around their centres of mass with application of Ising coupling parameter for the electrostatic interaction (appeared between carbonyl dipoles of neighbouring molecules) leads to the good agreement of the results with diffuse scattering observed in the X-ray analysis in the ranges of 1,6±0,1 nm in the *a* direction, 3,6±0,9 nm in *b* and 2,5±0,2 nm in *c*. Such a disorder in the scope of orientation disorder additionally reduces the correlation length in translational symmetry [18].

Possible existence of an additional interaction occurring in the anthrone, demonstrated by the presence of a higher boiling point in comparison to this one in anthraquinone (see Table 1), leads to increased conductivity of this compound in comparison to anthraquinone-despite the similar structure.

Therefore, the presence of such an interaction should be seen in the difference of properties of anthrone molecules in the solid state in comparison to their properties in the gas state. It would be natural to expect the differences in physical properties observed at the unit cell level for both anthrone and anthraquinone in relation to the same properties observed for a single molecule in the gas phase. The additional interaction between anthrone molecules should affect the value of the transfer integrals determining the probability of the charge carrier transfer between neighbouring molecules [19]. It just might be the reason for the increase of measurable electrical conductivity of anthrone in comparison to the electrical conductivity of anthraquinone.

We have conducted two step theoretical calculations with use TD-DFT in order to clarify this issue. In the first stage we have used quantum-mechanical calculations for determination the electronic structure and properties of a single molecule for both compounds. The calculations were made in the manner described in our previous paper [20]. In the second stage we have calculated the electronic structure and properties of a single crystal unit cell for both studied compounds. The results obtained in the second stage allowed us to describe intramolecular and intermolecular electron interactions for molecules situated in the equilibrium positions determined by a symmetry of the crystal unit cell. Such calculation allowed us to specify direction and value of the dipole moment of the single molecule and the single unit cell.

We have tried to made an analysis useful for evaluation the experimental values of the drift mobility for both studied compounds based on these calculations.

In the calculations we have used the convenient method applying for calculating excited states TD-DFT. The main merit of TD-DFT is presence of time dependent potential produced by electric field. Such TD-DFT external time-dependent potentials can be considered as a weak perturbation. Using this method, the dynamic process such as transition between two eigenstates can be described [21]. TD-DFT enables extraction of the information about excitation energies, frequency-dependent response properties and photo absorption spectra of the studied molecule. As is well known the polycyclic organics TD-DFT is compromise between accuracy and computational performance.

2. EXPERIMENT AND RESULTS

2.1. Experiment

We have used a special grade anthraquinone and anthrone (purified with zone melting) for experiment. Tests were carried out for measured cells "sandwich" type, i.e. in the shape of planar condenser filled with the studied hydrocarbon layer. The planar Au electrode was deposited on the glass substrate in the vacuum of the order of 10^{-5} Tr, and the semitransparent front electrode was made of Al. The substrate temperature during evaporation was around 300 K. The same conditions of vacuum thermal deposition for all tested samples provided the identity of the obtained structure of the layers for both studied materials, measured with use of the X-ray powder diffraction method.

Structural examinations of obtained anthrone and anthraquinone layers were made using X-ray diffraction with use of an automatic diffractometer DAR. The diffraction studies were made in the 2θ range from 5° to 80° with measuring step 0,05°.

The drift mobility for hole was determined for the layers of anthrone and anthraquinone with use of the time of flight method (TOF) exactly in the same manner as was described in detail in [22].

Performed measurements allowed us to make the comparative analysis of the mobility values in the anthrone and anthraquinone polycrystalline layers.

The mean values of the mobility of holes in the layers of anthrone were $(7\pm2)\cdot10^{-3}$ cm^2/Vs and for anthraquinone were $(8\pm2)\cdot10^{-4}$ cm^2/Vs.

It was difficult to explain the experimental difference in hole mobility values of approximately one order of magnitude according to similarity of the crystal structures of the layers.

2.2. Computational methodology

2.2.1. Calculation of molecules

The calculations were made with use TD-DFT which is one of the best known methods for calculation of exciting states, frequency – dependent response properties and photo absorption spectra of a given molecule. All calculations were carried out with GAUSSIAN 09 program [23]. It was performed using the PLATON project's infrastructure at the Technical

University of Lodz Computer Center. The structures of anthraquinone and anthrone were optimized using DFT at B3LYP (Becke three parameter (exchange), Lee Yang, and Parr) method using 6-311+g(d,p) basis set. The structure was considered completely optimized as stationary point was located and was confirmed by absence of imaginary frequencies. Based on the optimized geometric structure, the I.R, Raman, HOMO, LUMO and band gap calculations were performed with the same level of theory at the ground state. UV–Vis spectra were simulated with Time Dependent-Self Consistent Field method (TD-SCF) using B3LYP/6-311+g(d,p).

The optimized geometric structures with electrostatic potential map of the anthraquinone and anthrone molecules in the ground state are shown in the Fig. 2. The both structures were found to be planar, but the distribution of the atom charges in the anthrone molecule indicates the presence of dipole moment marked in the Fig. 2 by an arrow.

The same molecules in the crystal are still planar but distances between the corresponding atoms in the molecule are different when compare to the atoms in the molecule in the gas state [1, 2, 24].

Shortening of the lengths of the C-O bond was described in the [24] as the measure of an effect for the crystal field on the aromatic character of the molecules of the 27 derivatives of anthraquinone.

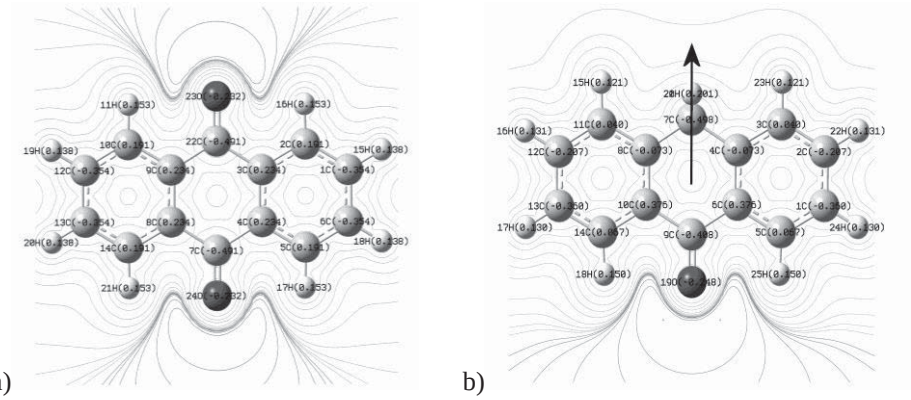

a) b)

Fig. 2. Electrostatic potential map of anthraquinone a) and anthrone b). The plots are calculated with DFT B3LYP/6-311+g(d,p) at ground state

In Tables 2 and 3 (atoms in the bonds in both tables are signed as in the Fig. 2). The comparison of the bond lengths obtained from our calculations with use of TD-DFT for a single molecule with the corresponding bond lengths inside the molecule obtained from X-ray diffraction in the crystal phase from the works

of Murty [2] for anthraquinone and Srivastava [1] for anthrone is shown. The effect of intermolecular interactions in the crystal structure is well seen in the shortening of the length of C-O bond for molecules of anthrone.

For anthrone this shortening is equal to 9.32%, but for anthraquinone is small and equals to 0.32%. This result indicates the greater influence of the crystal field on the molecule of anthrone then on the molecule of anthraquinone.

Table 2

Bond lengths for anthraquinone molecule in gas phase in comparison to the solid state

bond	TD-DFT	X-ray analysis [2]	$\Delta=10^3\cdot(\{1\}-\{2\})$	$W=10^2\cdot(\{3\}/\{1\})$
	[Å] {1}	[Å] {2}	[Å] {3}	[%] {4}
24O – 7C	1.220	1.224	4	0.32
7C – 4C	1.492	1.478	14	0.94
4C – 3C	1.406	1.372	34	2.41
3C – 22C	1.492	1.478	14	0.94
22C – 23O	1.220	1.224	4	0.03
4C – 5C	1.398	1.391	7	0.05
5C – 6C	1.390	1.372	18	1.29
6C – 1C	1.398	1.410	12	0.86
1C – 2C	1.390	1.372	18	1.29
2C – 3C	1.398	1.391	7	0,05

Table 3

Bond lengths for anthrone molecule in gas phase in comparison to the solid state

bond	TD-DFT	X-ray analysis [1]	$\Delta = 10^3\cdot(\{1\}-\{2\})$	$W = 10^2\cdot(\{3\}/\{1\})$
	[Å] {1}	[Å] {2}	[Å] {3}	[%] {4}
19O – 9C	1.223	1.109	114	9.32
9C – 6C	1.489	1.475	14	0.94
6C – 4C	1.402	1.391	11	0.78
4C – 7C	1.507	1.488	19	1.26
7C – 20H	1.097			
6C – 5C	1.404	1.389	15	1.07
5C – 1C	1.385	1.376	9	0.65
1C – 2C	1.399	1.364	35	2.50
2C – 3C	1.389	1.360	29	2.09
3C – 4C	1.401	1.412	11	0.79

2.2.2. Quantum-mechanical calculations of the crystal unit cell

The next stage of our work with use of TD-DFT was the calculation of the geometrical structure of molecules and the geometry of interactions between them in the crystal. The calculations were completed with the assumption that

the final 3D packing was matching point group symmetries. The calculations has been made with use of DFT B3LYP/sto-3g method. The calculation conducted for anthrone structure shows the convergence in the restricted scope. That caused the inability to obtain a global minimum for this structure.

Table 4

Bond lengths simulated for anthraquinone molecule in gas phase in comparison to bond lengths in molecule within simulated unit cell (atoms signed as in Fig. 2)

bond	TD-DFT for a molecule	TD-DFT for a unit cell	$\delta = 10^3 \cdot (\{1\} - \{2\})$	$W = 10^2 \cdot (\{3\}/\{1\})$
	[Å] {1}	[Å] {2}	[Å·10^{-3}] {3}	[%] {4}
24O – 7C	1.220	1.216	4	0,32
7C – 4C	1.492	1.500	8	0.54
4C – 3C	1.406	1.403	3	0,02
3C – 22C	1.492	1.500	8	0.54
22C – 23O	1.220	1.216	4	0.32
4C – 5C	1.398	1.385	13	0.93
5C – 6C	1.390	1.382	8	0.58
6C – 1C	1.398	1.390	8	0.58
1C – 2C	1.390	1.394	6	0.43
2C – 3C	1.398	1.382	15	1.07

Table 5

Bond length simulated for anthrone molecule in gas phase in comparison to bond lengths in molecule within simulated unit cell (atoms signed as in Fig. 2)

bond	TD-DFT for a molecule	TD-DFT for a unit cell	$\delta = 10^3 \cdot (\{1\} - \{2\})$	$W = 10^2 \cdot (\{3\}/\{1\})$
	[Å] {1}	[Å] {2}	[Å·10^{-3}] {3}	[%] {4}
19O – 9C	1.223	1.216	7	0,57
9C – 6C	1.489	1.500	11	0.74
6C – 4C	1.402	1.403	1	0.07
4C – 7C	1.507	1.403	104	6.90
6C – 5C	1.404	1.385	19	1.35
5C – 1C	1.385	1.382	3	0.22
1C – 2C	1.399	1.364	35	2.50
2C – 3C	1.389	1.394	5	0.36
3C – 4C	1.401	1.383	18	1.28

Tables 4 and 5 show the comparison of the bond lengths obtained from our calculations with use of TD-DFT for a single molecule in gas phase with the corresponding bond lengths inside the molecule obtained from simulations of the single crystal unit cell.

Above mentioned molecular calculations allowed us to determine the dipole moment in the crystal unit cell for both considered compounds. Calculated dipole moment in [*x*,*y*,*z*] axes system for anthraquinone has components [–0.48, –1.03, –1.70], and the value of the length of this vector is 2.04 Debye. For anthrone despite the "statistical" decomposition of molecules which is observed in the crystallographic measurements (taking into account the direction and the sense of the C-O bond) calculations showed the presence of a significant dipole moment. This dipol moment in relation to the axes [*x*,*y*,*z*] gives the value of components [17.51, 3.56, –0.70] leading to a value of 17.88 Debye for the length of this vector. The value of the dipole moment in the crystalline phase for the anthrone is thus 8.8 times higher than that for anthraquinone (see Fig. 3). This is almost exactly the same numerical value which can be calculated as the higher mobility of holes in the layers of anthrone in relation to the lower mobility of holes in the layers of anthraquinone.

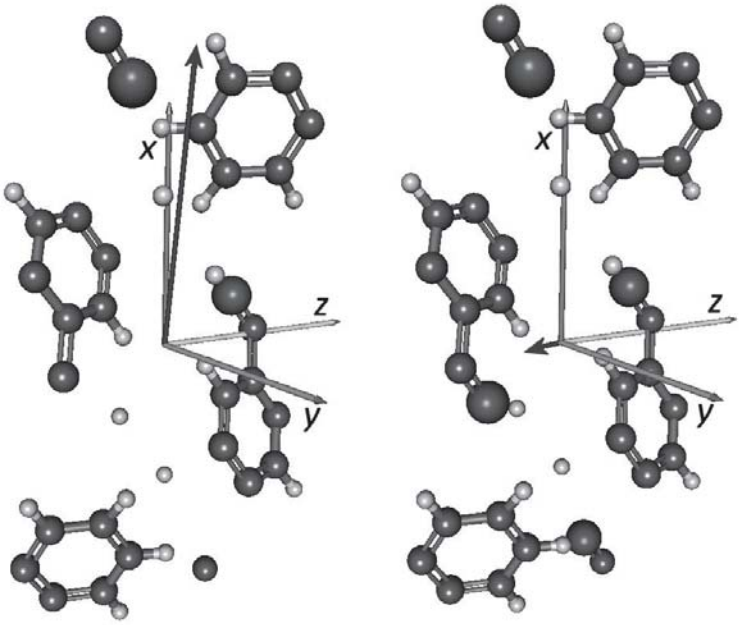

Fig. 3. Comparison of the value and direction of the dipol moments in the crystal phase for anthrone and anthraquinone, presented in *x*,*y*,*z* axes system

3. DISCUSSION AND CONCLUSIONS

In our simulation made with use of TD-DFT we have observed the changes in the bond lengths related to the interactions between molecules placed in the simulated unit cell. The changes in the corresponding bond lengths between carbons inside molecules in the gas phase and inside molecules in the simulated crystal unit cell (see Table 4 and 5) are also different for both considered compounds.

However, a clear change in length of the C-O bond in anthrone (Table 5) does not appear, in contrast to observed difference for anthrone molecules in the gas phase and in the real crystal as shown in Table 3.

This result indicates that the influence of the real crystal field (measured with X-ray diffraction) on the molecule is greater for the anthrone molecule than for anthraquinone one. Achieving such a result in the molecular calculations requires the consideration of a more complex model of calculations.

Above results demonstrate the influence of the assymetry of the anthrone molecule on the strenghthening of the effective crystal potential. This increase of the potential may favours the increase of the mobility in the anthrone layers.

The high microscopic dipole moment of a single crystal unit cell 17,88 D compared with a much smaller value of the macroscopic dipole moment 3.5 D for anthrone indicates that properties of this material can be considered as a function of the scale. Fact of existing dependence of the properties of anthrone on the scale is reflected in its high boiling point matched with its low melting point. High boiling point testifies to the strong interactions between nearest nighbours.

The little value of the microscopic dipole moments for a single molecule and for simulated single unit cell of anthraquinone compared to the little value of a macroscopic dipole moment indicates that properties of this material cannot be considered as a function of the scale.

Based on the obtained results the conclusions can be drawn, that the presence of the considerable value of dipole moment, in comparison to its lack for the anthraquinone layers is responsible for the increased mobility of anthrone layers. From our TD-DFT calculation it is seen that the presence of the permanent dipole moment for anthrone molecule has a direct impact on shaping the electronic structure of the unit cell, which leads to the permanent dipole moment calculated for crystal unit cell. The value of the dipole moment of 17,88 D calculated with TD-DFT for crystal unit cell is evidently different from mean dipole moment obtained from experiment which is 3.5 D. This phenomenon could explain the apparent discrepancy (seen in the Table 1)

between diminishing of the melting temperature with the simultaneous rise of the boiling temperature for anthrone in comparison to the anthracene.

Our TD-DFT calculations demonstrate that the presence of molecular dipole moment is responsible for different geometry of frontier orbitals in anthrone in comparison to adequate orbitals in anthraquinone. The shortening of the C-O bond in crystal phase [1,2] is much greater for anthrone, than for anthraquinone. This fact indicates an increase of the aromaticity of the anthrone skeleton in crystal [24], what can lead to greater delocalization of the π electrons and in consequence leads to the greater conductivity. The unique nature of interactions seen for non-centrosymmetrical molecules of anthrone may be considered as an effect of the presence of the dipole moment in the lowest triplet states. This may be responsible for greater charge mobility of anthrone [11,19,20].

Experimental values of the mobility in the room temperature for both molecular compounds in solid state are below 10^{-2} cm^2/Vs what indicates hopping transport. Activation energy for both compounds are very similar. Therefore, the magnitude of the hole mobility for anthrone, should be connected with greater level of the transfer integrals in comparison to the ones for anthraquinone. On the basis of this research it can be stated that the asymmetry seen in the electron distribution of the frontier orbitals in anthrone molecule is reflected in the emergence of a large dipole moment (17,88 D) in the volume of a single crystal unit cell. This fact cannot be observed by macroscopic methods because of statistical distribution of the dipole moment in the volume of the whole layer. However, the effect of microscopic interactions is reflected in the increased hole mobility for the anthrone in comparison to the anthraquinone.

ACKNOWLEDGEMENTS

We would like to express gratitude to prof. B. Marciniak and prof. M. Wieczorek for preparation of the spectral grade anthraquinone and anthrone and for enabling the X-ray analysis and to prof. J. Świątek for inspiring discussions.

The calculations presented in this paper are performed using the PLATON project's infrastructure at the Computer Center of Lodz University of Technology.

REFERENCES

[1] Srivastava S.N. 1964. Three-dimensional refinement of the structure of anthrone, Acta Cryst. 17:851-856.

[2] Murty B.V.R. 1960. Refinement of the structure of anthraquinone. Zeitschrift für Kristallographie. 113: 445-465.

[3] Karl N. 2003. Charge carrier transport in organic semiconductors. Synthetic Metals 133-134: 649-657.

[4] Di C., Zhang F., Zhu D. 2013. Multifunctional Integration of Organic Field-Effect Transistors (OFETs): Advances and Perspectives, Adv. Mater. 25: 313-330.

[5] Aleshin A.N., Lee J.Y., Chu S.W., Kim J.S., Park Y.W. 2004. Mobility studies of field effect transistor structures based on single crystals, Appl. Phys. Lett. 84: 5383-5385.

[6] Ostroverkhova O. 2016. Organic Optoelectronic Materials: Mechanisms and Applications, Chem. Rev. 116: 13279-13412.

[7] Hutchison G.R., Ratner M.A., Marks T.J. 2005. Intermolecular Charge Transfer between Heterocyclic Oligomers. Effects of Heteroatom and Molecular Packing on Hopping Transport in Organic Semiconductors, J. Am. Chem. Soc. 127:16866-16881.

[8] Köhler A., Bässler H. 2011. What controls triplet exciton transfer in organic semiconductors? J. Mater. Chem. 21: 4003-4011.

[9] Deng W-Q., Goddart III W.A. 2004. Predictions of hole mobilities in oligoacene organic semiconductors from quantum mechanical calculations. J. Phys. Chem. B 108:8614-8621.

[10] Rühle V., Lukyanov A., Falk M., Schrader M., Vehoff T., Kirkpatrick J., Baumeier B., Andrienko D. 2011. Microscopic Simulations of Charge Transport in Disordered Organic Semiconductors. J. Chem. Theory Comput. 7: 3335-3345.

[11] Bromley S., Illas F., Mas-Torrent M. 2008. Dependence of charge transfer reorganization energy on carrier localisation in organic molecular crystals. Phys. Chem. Chem. Phys. 10: 121-127.

[12] Rusu G.I. 1999-2000. Recent research in organic semiconductors. on the correlation between semiconductor characteristics and molecular structure of the compounds. Analele Stiintifice ale Universitatii "AL.I.CUZA" IASI Tomul XLV-XLVI, s. Fizica Stării Condensate. 229-241.

[13] Shimamori H., Houdo K., Uegaito H., Nakatani Y., Uchida K. 1989. Detection of Excited Triplet states of Aromatic Ketones and Determination of Their Dipole Moments by the Time-Resolved Microwave dielectric Absorption Technique. Chem. Soc. Jap. 8: 1379-1385.

[14] Angyal C.L., Le Fevre R.J.W. 1950. The polarities of enols. J. Chem. Soc. 106: 562-564.

[15] http://www.chemicalbook.com

[16] Flack H.D. 1970. I. Refinement and thermal expansion coefficients of the structure of anthrone (20-90°C) and comparison with anthraquinone. Phil. Trans. A 266: 561-574.

[17] Srivastava S.N. 1961. Diffuse layers in anthrone photographs. Acta Cryst. 14: 796-796.

[18] Reynolds P.A. 1975. A calculation of the molecular orientational disorder in crystalline anthrone. Acta Cryst. A31: 80-83.

[19] Small D.W., Matyushov D.V., Voth G.A. 2003. The theory of electron transfer reactions: What may be missing? J. Am. Chem. Soc. 125: 7470-7478.

[20] Kania S., Kościelniak-Mucha B., Kuliński J., Słoma P. 2015. Effect of molecule dipole moment on hole conductivity of polycrystalline anthrone and anthrachinone layers. Sci. Bull. Techn. Univ. Lodz, Physics 36: 13-26.

[21] Ong B.K., Woon K.L., Ariffin A. 2014. Evaluation of various density functionals for predicting the electrophosphorescent host HOMO, LUMO and triplet energies. Synth. Met. 195: 54-60.

[22] Kania S., Kondrasiuk J., Bąk G.W. 2004. Influence of ambient atmosphere on charge transport in polycrystalline thin films of three simple aromatic hydrocarbons. Eur. Phys. J. E. 15: 439-442.

[23] Gaussian 09, Revision A.02, Frisch M.J., Trucks G.W., Schlegel H.B., Scuseria G.E., Robb M.A., Cheeseman J.R., Scalmani G., Barone V., Mennucci B., Petersson G.A., Nakatsuji H., Caricato M., Li X., Hratchian H.P., Izmaylov A.F., Bloino J., Zheng G., Sonnenberg J.L., Hada M., Ehara M., Toyota K., Fukuda R., Hasegawa J., Ishida M., Nakajima T., Honda Y., Kitao O., Nakai H., Vreven T., Montgomery Jr. J.A., Peralta J.E., Ogliaro F., Bearpark M., Heyd J.J., Brothers E., Kudin K.N., Staroverov V.N., Kobayashi R., Normand J., Raghavachari K., Rendell A., Burant J.C., Iyengar S.S., Tomasi J., Cossi M., Rega N., Millam J.M., Klene M., Knox J.E., Cross J.B., Bakken V., Adamo C., Jaramillo J., Gomperts R., Stratmann R.E., Yazyev O., Austin A.J., Cammi R., Pomelli C., Ochterski J.W., Martin R.L., Morokuma K., Zakrzewski V.G., Voth G.A., Salvador P., Dannenberg J.J., Dapprich S., Daniels A.D., Farkas O., Foresman J.B., Ortiz J.V., Cioslowski J., Fox D.J., Gaussian, Inc., Wallingford CT, 2009.

[24] Kožíšek J., Breza M., Ulický L. 1993. Aromatic character of anthraquinone derivatives. Chem. Papers 47: 34-37.

WPŁYW SYMETRII ROZKŁADU ELEKTRONOWEGO CZĄSTECZKI NA MOMENT DIPOLOWY KOMÓRKI ELEMENTARNEJ I PRZEWODNICTWO CIENKICH WARSTW POLIKRYSTALICZNEGO ANTRONU I ANTRACHINONU

Streszczenie

Metodą TD-DFT obliczono strukturę elektronową cząsteczek oraz wartości momentu dipolowego komórek elementarnych dla antronu i antrachinonu. Zaobserwowano wpływ pola krystalicznego na zmianę długości wiązań w szkielecie antracenowym, który to obliczono metodą TD-DFT dla cząsteczek obu związków w fazie krystalicznej. Doświadczalnie określono wpływ obecności momentu dipolowego komórki elementarnej na ruchliwość dryftową nośników ładunków dla dwu aromatycznych związków wielo-pierścieniowych, antronu i antrachinonu krystalizujących w podobnej sieci krystalicznej $C_{2h}^5(P2_1/a)$, ale różniących się symetrią cząsteczki. W przypadku antronu, posiadającego niecentrosymetryczne cząsteczki, okazało się, że własności tego materiału są związane z jego rozmiarami. Mikroskopowe oddziaływania mające swoje odzwierciedlenie zarówno w wyznaczonej eksperymentalnie bardzo wysokiej temperaturze wrzenia, jak i w wynikach obliczeń momentu dipolowego pojedynczej komórki elementarnej antronu są związane z możliwością zwiększenia aromatyczności cząsteczek tego związku w fazie stałej. Wydaje się, że jest to przyczyną zwiększonej ruchliwości dziur w przypadku antronu w porównaniu do ruchliwości dziur w antrachinonie (o cząsteczkach centrosymetrycznych).